

Radioimmunotherapy with [¹³¹I]cG250 in Patients with Metastasized Renal Cell Cancer: Dosimetric Analysis and Immunologic Response

Adrienne H. Brouwers,¹ Wilhelmina C.A.M. Buijs,¹ Peter F.A. Mulders,² Pieter H.M. de Mulder,³ Wim J.M. van den Broek,¹ Carola Mala,⁴ Egbert Oosterwijk,² Otto C. Boerman,¹ Frans H.M. Corstens,¹ and Wim J.G. Oyen¹

Abstract Purpose: A study was designed to define the therapeutic efficacy, safety, and toxicity of two sequential high-dose treatments of radioimmunotherapy with [¹³¹I]cG250 in patients with metastasized renal cell carcinoma. Here, we report the dosimetric analysis and the relationship between the development of a human antichimeric antibody response and altered pharmacokinetics.

Experimental Design: Patients ($n = 29$) with progressive metastatic renal cell carcinoma received a low dose (222 MBq) of [¹³¹I]cG250 for dosimetric analysis, followed by the first radioimmunotherapy with 2,220 MBq/m² [¹³¹I]cG250 ($n = 27$) 1 week later. If no grade 4 hematologic toxicity was observed, a second low dose of [¹³¹I]cG250 ($n = 20$) was given 3 months later. Provided that no accelerated blood clearance was observed, a second radioimmunotherapy of [¹³¹I]cG250 was administered at an activity-dose level of 1,110 MBq/m² ($n = 3$) or 1,665 MBq/m² ($n = 16$). After each administration, whole-body images were obtained and the pharmacokinetics and the development of human antichimeric antibody responses were determined. Radiation-absorbed doses were calculated for whole body, red marrow, organs, and metastases.

Results: No correlation was found between hematologic toxicity and radiation-absorbed dose to the whole body or bone marrow, nor administered activity (MBq and MBq/kg). The tumor-absorbed doses varied largely. An inverse relation between tumor size and radiation-absorbed dose was found. Most tumor lesions received <10 Gy, whereas only lesions <5 g absorbed >50 Gy. A relatively high number of patients developed a human antichimeric antibody response (8 of 27) with altered pharmacokinetics, hampering additional radioimmunotherapies in four of these patients.

Conclusions: Dosimetric analysis did not adequately predict the degree of bone marrow toxicity. When human antichimeric antibody developed, the rapid clearance of radioactivity from the blood and body prohibited further treatment. According to the calculated absorbed dose in metastatic lesions, future radioimmunotherapy studies with radiolabeled cG250 should aim at treatment of small-volume disease or treatment in an adjuvant setting.

Renal cell carcinoma accounts for ~2% of all cancer deaths with almost 12,000 cancer deaths per year in the United States (1, 2). The only option for cure is (partial) nephrectomy. Once renal cell carcinoma has metastasized, chances for surviving the disease are grim; chemotherapy by itself has no effect (3) and radiotherapy is reserved for palliation only. Currently, immu-

notherapy with interleukin 2 and IFN- α , alone or in combination, is the only treatment with curative intent that is available for patients with metastatic renal cell carcinoma, although responses are modest and in the range of 5% to 25% (4, 5). Unfortunately, ~25% of the patients present with metastatic renal cell carcinoma, and up to half of the patients diagnosed with disease confined to the kidney, will ultimately develop metastases (6).

Because there is a need to develop new strategies for the treatment of metastatic renal cell carcinoma, we have been exploring radioimmunotherapy using monoclonal antibody (mAb) G250 in patients with metastatic renal cell carcinoma (7, 8). Oosterwijk et al. (9) showed the ability of radioiodinated murine antibody G250 to guide potentially high doses of radioactivity to renal cell carcinoma lesions. However, all patients developed human antimurine antibody, which was also observed by Divgi et al. (10) in a radioimmunotherapy study with mG250. Although no objective responses were observed, 17 of 33 evaluable patients had stable disease after one high-dose [¹³¹I]mG250 treatment. Because the efficacy of

Authors' Affiliations: Departments of ¹Nuclear Medicine, ²Urology, and ³Oncology, Radboud University Nijmegen Medical Centre, Nijmegen, the Netherlands; and ⁴Wilex AG, Munich, Germany

Grant support: Dutch Cancer Society (Koningin Wilhelmina Fonds), grant no. KUN99-1973, Ludwig Institute for Cancer Research (New York, NY; E. Oosterwijk), and Wilex A.G. (Munich, Germany).

Presented at the Tenth Conference on Cancer Therapy with Antibodies and Immunoconjugates, October 21-23, 2004, Princeton, New Jersey.

Requests for reprints: Adrienne H. Brouwers, Department of Nuclear Medicine, University Medical Center Groningen, P.O. Box 30001, NL-9700 RB Groningen, the Netherlands. Phone: 31-50-3613541; Fax: 31-50-3611712; E-mail: a.h.brouwers@nucl.umcg.nl.

©2005 American Association for Cancer Research.
doi:10.1158/1078-0432.CCR-1004-0010

radioimmunotherapy may be higher after repeated high-dose injections (11–13) and because repeated injections are mandatory for dosimetric studies preceding radioimmunotherapy, a chimeric version of G250 has been developed to reduce the immunogenicity of the antibody (7).

Several clinical studies with [¹³¹I]cG250 have been done (7, 8, 14–16). In a phase I activity dose-escalation study in 12 patients, the maximum tolerated dose in patients with progressive metastatic renal cell carcinoma disease was established at 2,220 MBq (60 mCi)/m² [¹³¹I]cG250 (8). In this study, stable disease was observed in one patient, whereas another patient showed a partial response (8). In a phase I clinical fractionated radioimmunotherapy with [¹³¹I]cG250, Divgi et al. (16) reported stable disease in 7 of 15 patients treated. Furthermore, these studies confirmed the reduced immunogenicity of the chimeric version of the antibody (7, 8, 15, 16).

In radioimmunotherapy, the bone marrow is the dose-limiting organ (17). It remains unclear whether the observed hematologic toxicities in an individual patient can be accurately predicted by the calculated radiation-absorbed dose to the bone marrow or whole body. For individual dosing, each radioimmunotherapy treatment is preceded by a tracer (low activity-dose) infusion of the radiolabeled mAb, followed by γ -radiation measurements and dosimetric calculations that requires extra efforts of patients, doctors, and dosimetrists involved.

A phase I/II study was designed to establish safety, response rate, and dosimetry of patients with progressive metastatic renal cell carcinoma treated with two high-dose radioimmunotherapies of [¹³¹I]cG250 to increase the antitumor effect. Both radioimmunotherapies were preceded by a tracer dose of [¹³¹I]cG250 for dosimetry to study the predictive value of these calculations for toxicity. Here, we report the dosimetric analysis and immunologic effects of repeated cG250 radioimmunotherapy.

Patients and Methods

Patients. Twenty-nine patients with clear cell renal cell carcinoma (median age 57 years, range 40–72 years, 20 males and 9 females) were included. All patients had undergone a tumor nephrectomy in the past and had measurable progressive disease at the time of enrollment. Patient characteristics and the inclusion and exclusion criteria are described in detail elsewhere (18). When patients did not complete the protocol, they were replaced. To detect a response rate of 30% (α , 0.05 and β , 0.20), 15 patients had to complete radiological and hematologic follow-up 3 months after the second radioimmunotherapy treatment of [¹³¹I]cG250 at maximum tolerated dose. The study was approved by the Medical Ethical Committee of the University Medical Center Nijmegen and the Institutional Review Board of the Ludwig Institute for Cancer Research. Before study entry, written informed consent was obtained from all patients.

Monoclonal antibody cG250 and radiolabeling. cG250 is a high-affinity ($K_a = 4 \times 10^9$ L/mol) chimeric, IgG1 mAb, reactive with the G250 antigen (7, 18). The isolation and immunohistochemical reactivity of mAb cG250 have been described elsewhere (7, 19). The G250 antigen has been identified as carbonic anhydrase isoenzyme 9 (MN/CA IX), a transmembranous glycoprotein (20–22). The antigen is expressed on the cell surface of the majority (>95%) of clear cell-type renal cell carcinomas (23). Approximately 80% of renal cell carcinomas are of the clear cell type. The reactivity of mAb cG250 to normal human tissues is restricted to the upper gastroin-

testinal mucosa and gastrointestinal-related structures (bile ducts, pancreas; refs. 19, 24).

Clinical-grade cG250 vials (5 mg/mL) were obtained from The Ludwig Institute for Cancer Research (New York, NY). mAb cG250 was radioiodinated with ¹³¹I (MDS Nordion, Fleurus, Belgium) according to the IodoGen method, using a remote system, as described previously (7, 8). The overall labeling efficiency of the remote radioiodination method ranged between 67% and 93% (mean 86%). The radiochemical purity of radiolabeled cG250 was determined by instant thin layer chromatography using instant thin layer chromatography silica gel strips (Gelman Sciences, Inc., Ann Arbor, MI) using 0.15 mol/L citrate buffer (pH 5.0) as the mobile phase. After purification, on average, 99.2% (range 95.3–99.9%) of the radioactivity in the antibody preparation was protein bound. Before each antibody administration, the immunoreactive fraction at infinite antigen excess of each preparation was determined on freshly trypsinized SK-RC-52 renal cell carcinoma cells essentially as described by Lindmo et al. (25) with minor modifications (7, 26). The immunoreactivity of the [¹³¹I]cG250 preparations used in this study was $94 \pm 5\%$.

Study design and radioimmunoscintigraphy. The present clinical trial was an uncontrolled phase I/II efficacy study of two radioimmunotherapy treatments with [¹³¹I]cG250, with both therapies given at the maximum tolerated dose (phase II). The maximum tolerated dose of the first radioimmunotherapy has been established previously and determined at 2,220 MBq (60 mCi)/m² (8). Because a second radioimmunotherapy of [¹³¹I]cG250 had not been given to patients previously, the maximum tolerated dose of the second radioimmunotherapy had to be established first (phase I). Three patients were included at the first dose level of radioimmunotherapy 2 of 1,110 MBq (30 mCi)/m²; all other patients were included at the next dose level of 1,665 MBq (45 mCi)/m², which was also the maximum tolerated dose of radioimmunotherapy 2. Both radioimmunotherapies were preceded with a tracer dose 1 week earlier to assess tumor uptake and for dosimetric analysis. Patients were monitored weekly after both radioimmunotherapies for adverse reactions and (hematologic) toxicity. Patients were evaluated for response (physical examination and computed tomography scan) 3 months after each radioimmunotherapy.

After both diagnostic i.v. infusion of [¹³¹I]cG250 [220 MBq (6 mCi), protein dose 5 mg (7), total volume 10 mL], four whole-body scintigraphic images were acquired directly and after 2 to 3, 4 to 5, and 7 days postinjection. The images were recorded using a double-headed γ -camera (MultiSpect 2, Siemens, Inc., Hoffman Estates, IL) equipped with parallel-hole high-energy collimators [symmetrical 15% window over 364 keV, scan speed 5 cm/min (days 0 and 2–3 postinjection) and 4 cm/min (days 4–5 and 7 postinjection)] and stored digitally in a 256 \times 1,024 matrix. Approximately 1 and 2 weeks after both radioimmunotherapies with [¹³¹I]cG250 (¹³¹I dosing depending on activity-dose level and body surface area, protein dose 5 mg, total volume 30–40 mL), additional whole-body scintigraphic images were recorded (scan speed 10 cm/min and 4–5 cm/min, respectively). To prevent excessive ¹³¹I uptake in the thyroid, patients received potassium iodide and potassium perchlorate.

Determination of human antichimeric antibody. To evaluate the immunogenicity of mAb cG250 after injection of cG250, the formation of human antichimeric antibody in all patients was tested retrospectively using ELISA as has been described previously (7, 8). Briefly, serum samples were incubated in mAb cG250-coated microtiter plates. After washing, peroxidase-conjugated cG250 was used as tracer antibody. Serial dilutions of anti-cG250 idiotype antibody NUH-91 IgG1 were used to obtain a standard curve (27). The lower quantification limit of the assay was 40 ng NUH-91/mL. cG250 human antichimeric antibody titers were expressed in ng/mL NUH-91 equivalents. Samples that contained human antichimeric antibody tested positive in at least two independent assay runs.

To identify the part of the chimeric murine/human G250 antibody to which the human antichimeric antibody response was directed, sera

that were positive in the sandwich ELISA described above were investigated in similar ELISAs with mG250, cMOv18, or cU36 coated on the plates instead of mAb cG250 (28, 29). The two chimeric mAbs, cMOv18 and cU36, have been produced using identical cDNAs encoding the constant regions of the human heavy and light chains of human IgG as used for producing cG250. In these assays, samples were tested before and after preabsorption with polyclonal murine IgG-coated dynabeads (Dyna, M-450 Epoxy, Oslo, Norway) to determine whether the anti-cG250 antibodies were directed against common epitopes on murine IgG or against unique epitopes of the G250 antibody. The results of these assays were classified as either positive or negative after correlation with the signal of the positive and negative control samples. Human antichimeric antibody were classified as anti-idiotypic, directed against the G250 antigen binding site, or as non-anti-idiotypic, directed against the human or murine framework of the chimeric antibody.

Serum samples were obtained before patients entered the study, after 3 months (before the second diagnostic [¹³¹I]cG250 infusion), and at 6 months after study entry. The frequency of sampling was increased when patients showed enhanced clearance of the radiolabel from the blood and body as an indication of the formation of human antichimeric antibody.

Dosimetry and pharmacokinetics. To estimate the radiation-absorbed dose to the patients (whole body), the organs, and the metastases delivered by the therapeutic injections, dosimetric analysis of the scintigraphic images following both diagnostic doses was done using the conjugated views counting technique with partial background subtraction and correction for attenuation and physical decay as described previously (30, 31). Briefly, region of interests over whole body, organs of interest, and metastases were drawn on the posterior and anterior scintigraphic images (32). Organs of interest, showing retention of the radiolabeled antibody on the anterior and posterior scintigraphic images, were lungs, heart, liver, spleen, remaining kidney, and thyroid. Only metastatic lesions that were identified and measurable on computed tomography and visualized on the scintigraphic images were analyzed. The volume of metastatic lesions was derived from computed tomography measurements using the formula π (length \times width \times height) / 6. It was assumed that 1 mL of metastatic tissue weighed 1 g. The activity in all region of interests was expressed as percentage of the total injected dose.

Subsequently, the residence times of activity in whole body and organs of interest were calculated using monoexponential curve fitting because uptake in these region of interests decreased with time. The residence times of thyroid and metastases were calculated using trapezoidal curve fitting because uptake in these regions increased with time. Radiation-absorbed doses to organs and metastases were calculated with the MIRDOSE3 program (Oak Ridge Associated Universities, Oak Ridge, TN) using the adult male phantom for men, adult female phantom for women, using the dynamic bladder model (fraction is 1, bladder voiding at 4-hour interval), and using the nodule module for metastases with iteration of metastatic weight to calculate the corresponding rad/ μ Ci-h (33). The residence time of and the radiation-absorbed dose to the bone marrow were calculated by a blood-derived method as described by Shen et al. (34). All absorbed doses were expressed either in mGy/MBq or Gy.

Whole-body retention of the radiolabel was also measured directly 4 hours and 2 to 3, 4 to 5, and 7 days postinjection of a diagnostic [¹³¹I]cG250 infusion using a scintillation crystal at 3.7 m from the patient according to the method described by Divgi et al. (16). During hospitalization, after infusion of a [¹³¹I]cG250 radioimmunotherapy, whole-body retention was measured daily until discharge. The clearance rate of the [¹³¹I]cG250 radiolabel from the whole body after both diagnostic and radioimmunotherapy infusions was calculated using linear curve fitting and by this the number of hours required for 50% of the activity to be effectively removed from the whole-body ($t_{1/2}$ eff) was determined. These data were also used to calculate the absorbed dose to

the whole body and the results were compared with the whole-body absorbed dose derived from the serial γ -camera images.

Plasma samples were drawn directly 30, 60, 90, 120, and 240 minutes, and 2 to 3, 4 to 5, and 7 days postinjection of a diagnostic [¹³¹I]cG250 infusion and at 30 and 180 minutes, and 2 to 3, 4 to 5, and 6 to 7 days postinjection of a [¹³¹I]cG250 radioimmunotherapy dose. Pharmacokinetics data were analyzed as described previously (7). Clearance rates of [¹³¹I]cG250 from the circulation were calculated using the nonlinear least-squares regression analysis. Based on these curves, the time required for 50% of the activity to be removed from the blood ($t_{1/2}$) in the distribution phase (α) and elimination phase (β) was determined.

Both the clearance rates from plasma and whole body were used to detect rapid clearance of radioactivity from the blood and body due to immune complex formation induced by human antichimeric antibody. Clearance rates after the first diagnostic [¹³¹I]cG250 infusion served as baseline for each patient, so a difference in clearance rate after a subsequent injection of [¹³¹I]cG250 could be accurately detected for the individual patient.

Statistical analysis. Statistical analysis of the pharmacokinetic data was done using Bonferroni-corrected, repeated measures one-way ANOVA. Scatter plots were generated to determine whether a significant correlation (Pearson correlation test) existed between observed hematologic toxicity and the various calculated dosimetric parameters, between whole-body, radiation-absorbed dose measured with the γ -camera (MIRDOSE3) versus the γ -probe, and also between the clearance rate of the radiolabel derived from the whole-body measurements versus blood samples. Differences were considered significant when $P < 0.05$ (two-sided). All values are expressed as mean \pm SD unless stated otherwise.

Results

Patients. Two of the 29 patients who were injected with the first tracer dose of [¹³¹I]cG250 were excluded from further evaluation, including human antichimeric antibody and dosimetry, due to preliminary exclusion from the study (18). Nine of the 27 patient data sets were incomplete; these patients were taken off study because of grade 4 hematologic toxicity after radioimmunotherapy 1 ($n = 3$), because of rapid progressive disease ($n = 2$), or because of the development of a human antichimeric antibody response with rapid clearance of the radiolabel from blood and body ($n = 4$) (18). If possible, the incomplete data sets were used in the evaluations, along with the complete data sets: three patients at the first dose level of radioimmunotherapy 2, and 15 patients who received radioimmunotherapies 1 and 2 at their respective maximum tolerated doses (maximum tolerated dose of radioimmunotherapy 2 [1,665 MBq (45 mCi)/m²] was 75% of the maximum tolerated dose of radioimmunotherapy 1 [2,220 MBq (60 mCi)/m²] due to dose-limiting hematologic toxicity) (18). Of the three patients who received 2,220 and 1,110 MBq/m² for radioimmunotherapies 1 and 2, respectively, one patient showed stable disease, whereas the other two patients remained progressive. Of the 15 patients who received radioimmunotherapies 1 and 2 at the respective maximum tolerated doses, previously progressive disease stabilized in four patients, whereas 11 patients remained progressive (18).

Determination of human antichimeric antibody. The human antichimeric antibody titers of the patients who developed a detectable human antichimeric antibody response are shown in Table 1. Besides four patients (patients 9, 10, 11, and 25) who were excluded from the study due to enhanced clearance of the radiolabel from the blood and body caused by the presence of

Table 1. Relationship between human antichimeric antibody response and blood clearance of [¹³¹I]cG250

Patient no.	HACA titer*									Blood clearance [†]
	Pre [‡]	RIT 1 [§]	Months after RIT 1			RIT 2	Months after RIT 2			
			1	2	3 [¶]		1	2	3	
1	neg	n.d.	n.d.	n.d.	<u>63</u>	n.d.	n.d.	n.d.	neg	52.0
9	neg	n.d.	n.d.	n.d.	<u>350</u>	358	6,146	1,032	278	22.0
10	neg	<u>93</u>	704	1,324	l.f.	l.f.	l.f.	l.f.	l.f.	20.5
11	neg	neg	neg	n.d.	<u>114</u>	n.d.	178,783	l.f.	l.f.	22.0
14	neg	neg	neg	n.d.	<u>47</u>	neg	245	350	327	59.1
21	neg	neg	neg	neg	neg	<u>neg</u>	neg	n.d.	634	74.0
25	neg	<u>890</u>	57,893	l.f.	l.f.	l.f.	l.f.	l.f.	l.f.	26.9
27	neg	neg	n.d.	60	103	<u>neg</u>	355	n.d.	240	51.9

Abbreviations: HACA, human antichimeric antibody; RIT, radioimmunotherapy; neg, negative; n.d., not determined; l.f., lost to follow-up.

*Human antichimeric antibody titers in ng/mL NUH-91 equivalents.

[†] Blood clearance as $t_{1/2\beta}$ in hours. Blood clearance was measured at Pre, RIT 1, 3 months after RIT 1 and at RIT 2. Only one value of blood clearance per patient is shown. The depicted blood clearance corresponds to the underlined human antichimeric antibody titer.

[‡] Tracer 1 was given before (pre) radioimmunotherapy 1.

[§] One week after tracer 1.

^{||} One week after tracer 2.

[¶] Tracer 2 was given 3 months after radioimmunotherapy 1.

human antichimeric antibody, detectable human antichimeric antibody titers developed in an additional four patients (patients 1, 14, 21, and 27) during course of the study. Patients 1, 14, and 21 developed a human antichimeric antibody response relatively late (>1 month after radioimmunotherapy) and/or showed relatively low human antichimeric antibody titers and no enhanced clearance of injected mAb cG250 was detected at the time of radioimmunotherapy injection. In contrast, patients 10, 11, and 25, who developed high human antichimeric antibody titers before radioimmunotherapy 2 was administered, showed enhanced clearance of the preceding dose (Table 1). Once clinically relevant (associated with a markedly enhanced blood clearance of the radiolabel) human antichimeric antibody titers had developed, human antichimeric antibody remained detectable in serum for at least the duration of the follow-up period (Table 1).

Whether a patient would develop human antichimeric antibody could not be derived from the scheme of the previous cG250 injections (patients 25 and 27 both had mAb cG250 infusions before study entry; whereas patient 25 did show enhanced clearance, patient 27 did not), the number of cG250 injections (human antichimeric antibody became detectable after two to four cG250 infusions), the interval of human antichimeric antibody development after the last cG250 injection (ranging from 1 week to 3 months), or the presence of detectable human antichimeric antibody at the time of the next cG250 infusion (patients 9-11, 25 enhanced clearance versus patients 1, 14, 21, and 27, no enhanced clearance;

merit antibody remained detectable in serum for at least the duration of the follow-up period (Table 1). Whether a patient would develop human antichimeric antibody could not be derived from the scheme of the previous cG250 injections (patients 25 and 27 both had mAb cG250 infusions before study entry; whereas patient 25 did show enhanced clearance, patient 27 did not), the number of cG250 injections (human antichimeric antibody became detectable after two to four cG250 infusions), the interval of human antichimeric antibody development after the last cG250 injection (ranging from 1 week to 3 months), or the presence of detectable human antichimeric antibody at the time of the next cG250 infusion (patients 9-11, 25 enhanced clearance versus patients 1, 14, 21, and 27, no enhanced clearance;

Table 2. Radiation-absorbed dose in whole body, organs, and metastases in men

Organs	Radiation-absorbed dose* (n = 16) [†]			Radiation-absorbed dose (n = 13) [‡]		
	Mean ± SD	Minimum	Maximum	Mean ± SD	Minimum	Maximum
Heart wall	0.51 ± 0.11	0.24	0.73	0.55 ± 0.09	0.42	0.70
Lungs	0.58 ± 0.09	0.45	0.80	0.59 ± 0.11	0.46	0.86
Liver	0.64 ± 0.04	0.57	0.75	0.68 ± 0.15	0.49	1.00
Spleen	0.98 ± 0.40	0.23	1.52	1.00 ± 0.47	0.23	1.81
Kidneys	1.01 ± 0.30	0.61	1.56	1.05 ± 0.40	0.64	1.78
Thyroid	2.21 ± 0.76	0.85	3.40	2.19 ± 0.84	0.82	3.54
Bone marrow	0.39 ± 0.06	0.31	0.54	0.38 ± 0.04	0.32	0.46
Testes	0.22 ± 0.03	0.14	0.28	0.22 ± 0.03	0.18	0.29
Whole body	0.28 ± 0.03	0.21	0.33	0.28 ± 0.04	0.24	0.37
Metastases [§]	2.09 ± 2.67	0.11	15.7	2.74 ± 3.06	0.21	16.4

*Radiation-absorbed dose in mGy/MBq.

[†] After the first diagnostic [¹³¹I]cG250 infusion.

[‡] After the second diagnostic [¹³¹I]cG250 infusion, 3 months later.

[§] After the first diagnostic infusion, 58 metastatic lesions were evaluated, of which 41 were also evaluable after the second diagnostic infusion.

Table 3. Radiation-absorbed dose in whole body, organs, and metastases in women

Organs	Radiation-absorbed dose* (<i>n</i> = 7) [†]			Radiation-absorbed dose (<i>n</i> = 5) [‡]		
	Mean ± SD	Minimum	Maximum	Mean ± SD	Minimum	Maximum
Heart wall	0.66 ± 0.14	0.50	0.82	0.61 ± 0.16	0.44	0.84
Lungs	0.81 ± 0.18	0.54	1.01	0.78 ± 0.19	0.53	0.94
Liver	0.85 ± 0.06	0.77	0.95	0.79 ± 0.11	0.67	0.95
Spleen	1.28 ± 0.27	0.78	1.60	1.22 ± 0.44	0.53	1.74
Kidneys	1.09 ± 0.67	0.33	2.09	1.43 ± 0.33	1.05	1.79
Thyroid	2.36 ± 0.38	1.74	2.72	2.68 ± 0.11	2.37	2.82
Bone marrow	0.43 ± 0.08	0.33	0.53	0.41 ± 0.12	0.28	0.60
Ovaries	0.36 ± 0.04	0.31	0.42	0.31 ± 0.08	0.22	0.41
Uterus	0.34 ± 0.04	0.30	0.42	0.32 ± 0.08	0.23	0.42
Whole body	0.36 ± 0.04	0.31	0.41	0.33 ± 0.08	0.23	0.42
Metastases [§]	13.1 ± 23.1	0.12	105	5.66 ± 8.35	0.16	39.8

*Radiation-absorbed dose in mGy/MBq.

[†]After the first diagnostic [¹³¹I]cG250 infusion.

[‡]After the second diagnostic [¹³¹I]cG250 infusion, 3 months later.

[§]After the first diagnostic infusion, 38 metastatic lesions were evaluated, of which 28 were also evaluable after the second diagnostic infusion.

Table 1). Thus, no pattern could be discerned as to which patient was at risk to develop a human antichimeric antibody response.

Human antichimeric antibody responses were predominantly anti-idiotypic, as the human antichimeric antibody could not be absorbed using murine IgG-coated beads, and the samples were negative in the catcher ELISA using chimeric (cU36 and cMOv18) antibodies. Patient 1 displayed a human antichimeric antibody response against the human framework of the cG250 antibody because samples of this patient were also positive when cU36 or cMOv18 were used as catcher antibody (data not shown).

Dosimetry and pharmacokinetics. The estimated mean radiation-absorbed dose of [¹³¹I]cG250 in total body, organs, and metastases based on the images acquired after the first and second diagnostic [¹³¹I]cG250 infusion are shown in Tables 2 (men) and 3 (women). The data for men and women are presented separately, as two different phantom models (male and female) were used in MIRDOSE3 and blood-derived assessment of absorbed dose to the red marrow. For normal tissues, the calculated absorbed dose based on the first diagnostic infusion was highly similar to the calculated absorbed dose based on the second diagnostic infusion that was administered 3 months later. Visually, the highest uptake was observed in thyroid and metastatic lesions corresponding with the quantitatively determined highest radiation-absorbed doses (Tables 2 and 3).

The observed platelet toxicity did not correlate with the radiation-absorbed dose to the bone marrow, the absorbed dose to whole body, or the administered activity (in MBq or MBq/kg; Fig. 1). Similarly, no significant correlation was found between the observed leukocyte toxicity and radiation-absorbed dose to the bone marrow and whole body or administered activity (data not shown).

Absorbed dose in metastases varied widely, but did not exceed 10 Gy for most lesions (Fig. 2). The computed tomography-derived median weight of metastatic lesions was 17.5 g, range 0.1 to 335 g (*n* = 91). There was a significant correlation between

absorbed doses and weight of the metastatic lesions (*r* = 0.63, *P* < 0.001) with the highest radiation-absorbed doses guided to the smaller metastases (<5 g). However, this did not correlate with a better response percentage of these lesions; no difference in response (≥25% regression) or stabilization (<25% regression or <25% progression) between small (~2 g tissue) and larger metastases was found (data not shown).

The radiation-absorbed dose to the whole body measured with the γ -probe after a radioimmunotherapy injection of [¹³¹I]cG250 was in good agreement (*r* = 0.74 and *r* = 0.81 for radioimmunotherapies 1 and 2, respectively) with the radiation-absorbed dose to the whole body estimated by MIRDOSE3-based estimates using the region of interest of the whole body (Fig. 3A and B). Also, there was a good correlation (*r* = 0.93 and *r* = 0.85) between the clearance rates of the radiolabel expressed as $t_{1/2} \beta$ derived from the blood sampling and $t_{1/2} \text{eff}$ derived from the probe measurements after both radioimmunotherapies (Fig. 3C and D).

In patients with no or low positive human antichimeric antibody titers, clearance of the radiolabel from the blood after the second, third, or fourth injection of [¹³¹I]cG250 was not significantly different from the first injection (*P* = 0.77 for $t_{1/2} \alpha$, *P* = 0.35 for $t_{1/2} \beta$). After a tracer injection, half-life of the distribution phase ($t_{1/2} \alpha$) was 6.8 ± 2.4 hours and the half-life of the elimination phase ($t_{1/2} \beta$) was 58.0 ± 9.4 hours. After a radioimmunotherapy injection, $t_{1/2} \beta$ was 61.3 ± 10.2 hours ($t_{1/2} \alpha$ could not be reliably assessed). In contrast, a fast clearance of the radiolabel from the blood was noted in patients with highly elevated human antichimeric antibody titers (Table 1).

Discussion

In this study, dosing of the administered radioactivity based on body surface area at maximum tolerated dose resulted in hematologic toxicities ranging from none to grade 4. No correlation was observed between myelotoxicity and the

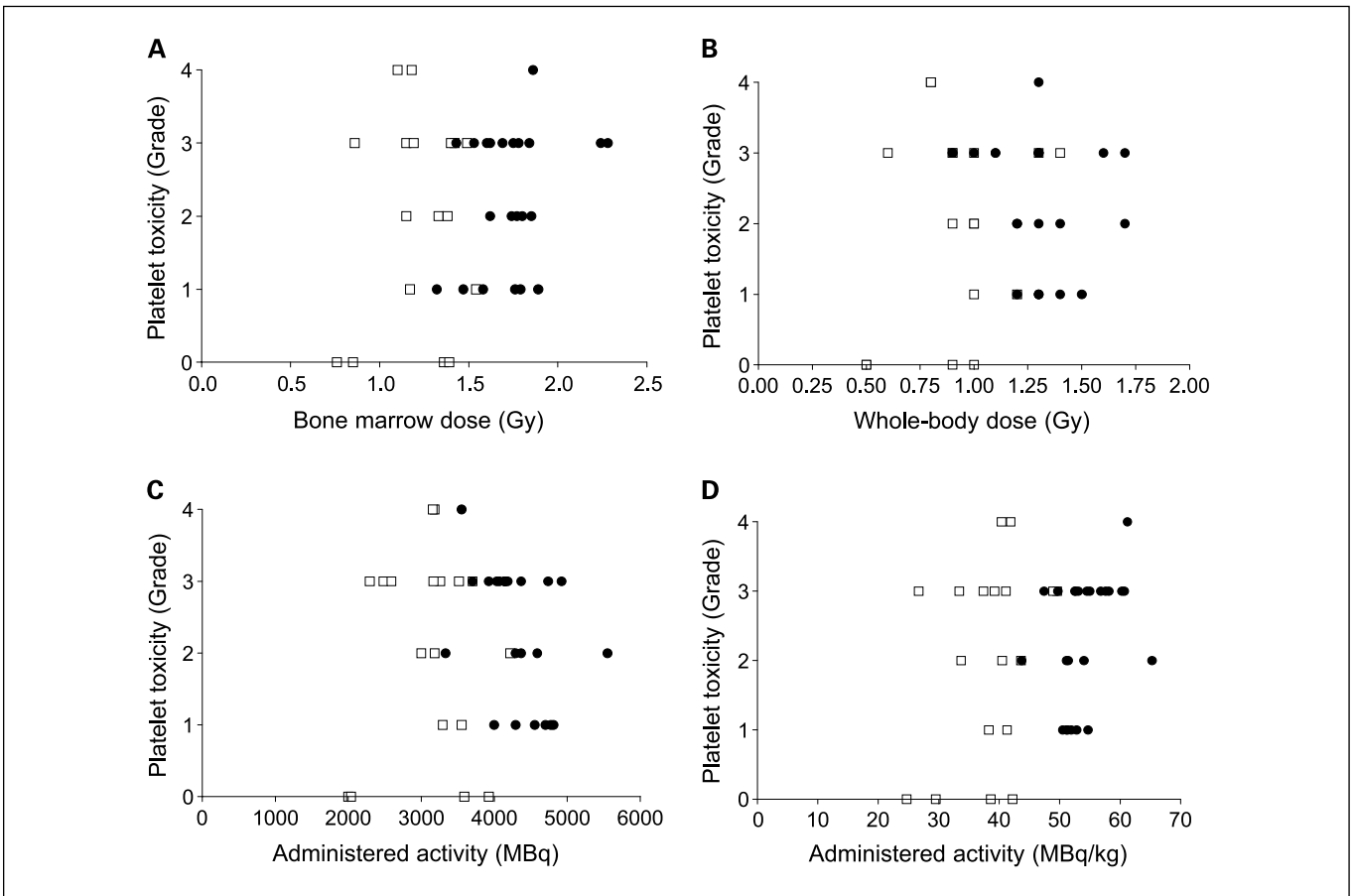


Fig. 1. Scatterplots of platelet toxicity grade versus radiation-absorbed dose to bone marrow (A), radiation-absorbed dose to whole body (B), and administered activity in MBq (C) or MBq/kg (D) after radioimmunotherapy 1 (●) or radioimmunotherapy 2 (□). No significant correlation was detected; *r* varied between -0.39 and 0.36 .

radiation-absorbed dose to the bone marrow or whole body or other parameters (administered activity in MBq/kg or MBq). Various studies reported that dosimetric estimations do not very well predict the severity of toxicity or the outcome of therapy (11, 35, 36), although in some studies fairly good correlations for these parameters are reported (10, 37, 38). We also could not predict hematologic toxicity for the individual patients treated with two radioimmunotherapies of [¹³¹I]cG250 at maximum tolerated dose. This is remarkable as the patients in this study were not heavily pretreated with chemotherapy. Thus, at this point, activity dosing based on conventional dosimetric analysis of a tracer injection that adequately predicts susceptibility for significant hematologic toxicity is not feasible (39). This may change when more accurate dosimetric calculations based on single-photon emission computed tomography or positron emission tomography can be applied (40–42). However, it is possible that no correlation between the radiation-absorbed dose and the currently used toxicity parameters exists and that, in the future, the variable radiosensitivity of the bone marrow should be taken into account as postulated by Blumenthal et al. (43).

As expected, there was a good correlation between the whole body-absorbed dose estimates derived from the γ -camera-based method (MIRDSE3) and the method using the γ -probe. Thus, whole body radiation-absorbed dose can

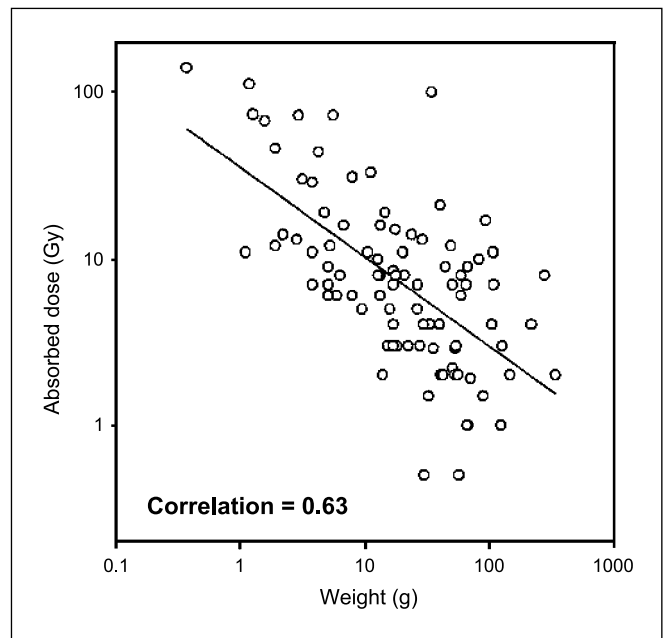


Fig. 2. Absorbed dose in metastases after radioimmunotherapy 1 plotted against weight of metastatic lesions on logarithmic scales. The smallest lesions received the highest radiation-absorbed doses ($r = 0.63$, $P < 0.001$).

be reliably measured with the γ -probe after a therapeutic dose of [^{131}I]cG250. Because this is a fast, more patient-friendly method requiring less recording and processing time, it could serve as an alternative for the γ -camera-based method. As such, it is being used after a diagnostic dose of ^{131}I -labeled murine anti-CD-20 ([^{131}I]tositumomab; Bexxar) in the treatment of non-Hodgkin's lymphoma to establish the dose of the therapeutic injection that delivers a fixed number of absorbed dose to the whole body (75 cGy in patients with normal pretreatment platelet counts; ref. 43). Furthermore, the γ -probe method provides estimates for whole body-absorbed dose in the first days after radioimmunotherapy with a radioiodinated antibody, which cannot be achieved with a γ -camera as patients are confined to their rooms for radiation safety reasons. Likewise, blood sampling after a therapeutic dose of [^{131}I]cG250 may be replaced by γ -probe measurements because there is a high correlation between the clearance rates of the radiolabel derived from blood sampling ($t_{1/2 \beta}$) and the probe measurements ($t_{1/2 \text{ eff}}$) after radioimmunotherapies. It would not only reduce frequent blood sampling but also avoid additional radiation exposure for the medical staff.

In the present study, the radiation doses that were delivered to the normal tissues were very consistent after radioimmunotherapies 1 and 2 according to MIRDOSE3 calculations. Despite adequate thyroid blockage, the thyroid was the organ with the highest radiation-absorbed dose. The mean radiation-absorbed dose in metastases was generally higher than in normal tissues corresponding with the good visual uptake of [^{131}I]cG250 in metastatic lesions on the [^{131}I]cG250 scans, but variation in absorbed dose in metastases varied widely, due to small patient numbers and interpatient/lesion variation, especially in our female patients. However, the radiation-absorbed doses that were delivered to the larger tumors generally did not exceed 10 Gy. This is well below the minimum of 50 Gy considered to be required for a therapeutic response in most malignancies (17). Like others (11, 45), we also observed an inverse relationship between tumor size and mAb uptake in the tumors, resulting in higher radiation doses guided to the smaller (<5 g) tumor lesions. Therefore, there is room for improvement of radioimmunotherapy with cG250 in renal cell carcinoma patients by changing the setting to treatment of small volume disease or by applying radioimmunotherapy in an adjuvant setting.

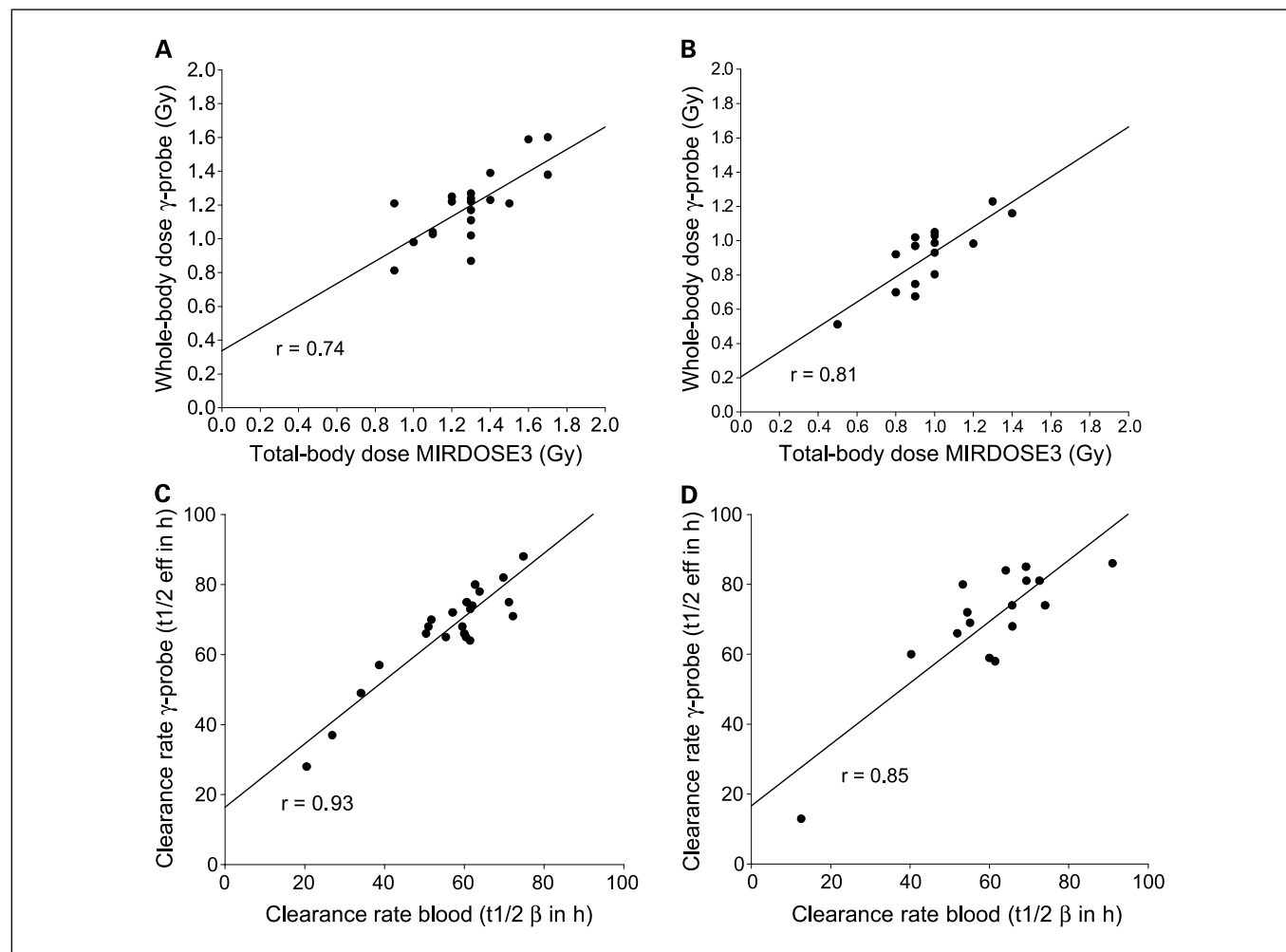


Fig. 3. Scatterplots of radiation-absorbed dose of the whole body measured with a γ -camera (MIRDOSE3) versus whole body-absorbed dose measured with a γ -probe after radioimmunotherapy 1 (A) and radioimmunotherapy 2 (B), and of clearance rate of [^{131}I]cG250 derived from blood sampling versus γ -probe measurements after radioimmunotherapy 1 (C) and radioimmunotherapy 2 (D). Correlation was highly significant ($P = 0.0002$ for A and B, and $P < 0.001$ for C and D).

In an unexpectedly high number of patients, elevated human antichimeric antibody titers were observed (8 of 27 patients). Serum conversions were observed early (within a week after cG250 infusion), but also appeared later. When human antichimeric antibody resulted in accelerated clearance of the radiolabeled antibody (4 of 27 patients), the human antichimeric antibody response interfered with effective targeting of the tumor lesions. Both γ -probe measurements and blood sampling proved very helpful to indicate in which patients human antichimeric antibody developed. All four patients with accelerated clearance of the radiolabel had markedly elevated human antichimeric antibody titers. This is in line with the observations of Divgi et al. (16) in the fractionated dose-escalation study with [¹³¹I]cG250 who observed altered clearance of the radiolabeled antibody in two patients, accurately correlating with the presence of human antichimeric antibody.

In a previous radioactivity dose-escalation study with [¹³¹I]cG250, only 1 of 12 patients developed elevated human antichimeric antibody titers (8). This particular patient had already received cG250 infusions in a previous study (8). Studies with unlabeled cG250 reported human antichimeric antibody development in only very few patients. In a phase I protein dose-escalation study (cG250 protein dose of 5-10 to 25-50 mg/m²) in which patients with renal cell carcinoma received multiple injections with mAb cG250, human antichimeric antibody was detected in 1 of 12 patients (46). Furthermore, in a European multicenter phase II trial in 36 patients, only two patients developed human antichimeric antibody (47). In the latter study, progressive renal cell carcinoma patients were treated with weekly doses of 50 mg of unconjugated cG250 for 12 cycles. Both serum conversions occurred relatively late (≥ 12 weeks after start treatment). Therefore, the enhanced incidence of human antichimeric antibody observed in our study are most likely related to the particular protein dose and/or timing of the injections used in this study. Interestingly, 5 of 12 patients with squamous cell carcinoma of head and neck that received the radiolabeled chimeric antibody cU36 developed human antichimeric antibody responses when injected with a tracer dose (2 mg)

followed by a radioimmunotherapy dose [12 mg ($n = 2$) or 52 mg ($n = 10$)] 1 week later (48), also suggesting that the current protein administration schedule could be particularly immunogenic.

In conclusion, in these radioimmunotherapy studies, no correlation was observed between observed hematologic toxicity and calculated absorbed dose to whole body or bone marrow, nor administered activity in MBq and MBq/kg. Currently, there is no apparent reason to change to an individual-based dosing scheme for future radioimmunotherapy trials with [¹³¹I]cG250. Human antichimeric antibody developed in 8 of 27 patients, preventing further treatment in 4 of 27 patients because of accelerated clearance of radiolabeled antibody from the blood. An enhanced clearance rate of the radiolabel from the blood and body (detected either by frequent blood sampling or whole-body dose measurements with a γ -probe) accurately predict the presence of high human antichimeric antibody levels at the time of injection. Immunogenicity of cG250 was higher compared with previous treatment schedules using ¹³¹I-labeled or unlabeled cG250, most likely due to differences in protein dosing and/or timing. This should be considered in future radioimmunotherapy studies with mAb cG250. In most patients, the humoral human antichimeric antibody response was anti-idiotypic. It remains to be shown whether humanizing the G250 antibody (grafting CDRs in a human IgG framework) will further reduce the immunogenicity of the antibody. As sufficiently high absorbed doses were only calculated for small metastatic lesions, future radioimmunotherapy studies with radiolabeled cG250 should aim at treatment of small volume disease or treatment in an adjuvant setting.

Acknowledgments

We thank Volker Boettger (Wilex A.G., Munich, Germany) and Julliette van Eerd (Department of Nuclear Medicine, Radboud University Nijmegen Medical Centre, Nijmegen, the Netherlands) for performing the ELISA tests to determine the human antichimeric antibody responses, and Paul Krabbe, Ph.D. (Department of Medical Technology Assessment, Radboud University Nijmegen Medical Centre, Nijmegen, the Netherlands), for giving statistical advice.

References

1. Incidence of cancer in the Netherlands 1998. In: Visser O, Coebergh JWW, Schouten LJ, van Dijk JAAM, editors. Utrecht (the Netherlands): Vereniging van Integrale Kankercentra; 2002.
2. Greenlee RT, Murray T, Bolden S, Wingo PA. Cancer statistics, 2000. *CA Cancer J Clin* 2000;50:7-33.
3. Yagoda A, Petrylak D, Thompson S. Cytotoxic chemotherapy for advanced renal cell carcinoma. *Urol Clin North Am* 1993;20:303-21.
4. Negrier S, Escudier B, Lasset C, et al. Recombinant human interleukin-2, recombinant human interferon alfa-2a, or both in metastatic renal-cell carcinoma. *N Engl J Med* 1998;338:1272-8.
5. Fisher RI, Rosenberg SA, Fyfe G. Long-term survival update for high-dose recombinant interleukin-2 in patients with renal cell carcinoma. *Cancer J Sci Am* 2000;6:55-7s.
6. Savage PD. Renal cell carcinoma. *Curr Opin Oncol* 1996;8:247-51.
7. Steffens MG, Boerman OC, Oosterwijk-Wakka JC, et al. Targeting of renal cell carcinoma with iodine-131-labeled chimeric monoclonal antibody G250. *J Clin Oncol* 1997;15:1529-37.
8. Steffens MG, Boerman OC, de Mulder PH, et al. Phase I radioimmunotherapy of metastatic renal cell carcinoma with ¹³¹I-labeled chimeric monoclonal antibody G250. *Clin Cancer Res* 1999;5:3268-74s.
9. Oosterwijk E, Bander NH, Divgi CR, et al. Antibody localization in human renal cell carcinoma: a phase I study of monoclonal antibody G250. *J Clin Oncol* 1993;11:738-50.
10. Divgi CR, Bander NH, Scott AM, et al. Phase I/II radioimmunotherapy trial with iodine-131-labeled monoclonal antibody G250 in metastatic renal cell carcinoma. *Clin Cancer Res* 1998;4:2729-39.
11. Behr TM, Sharkey RM, Juweid ME, et al. Phase I/II clinical radioimmunotherapy with an iodine-131-labeled anti-carcinoembryonic antigen murine monoclonal antibody IgG. *J Nucl Med* 1997;38:858-70.
12. Behr TM, Liersch T, Greiner-Bechert L, et al. Radioimmunotherapy of small-volume disease of metastatic colorectal cancer. *Cancer* 2002;94:1373-81.
13. Ychou M, Pelegrin A, Faurous P, et al. Phase-I/II radio-immunotherapy study with iodine-131-labeled anti-CEA monoclonal antibody F6 F(ab')₂ in patients with non-resectable liver metastases from colorectal cancer. *Int J Cancer* 1998;75:615-9.
14. Steffens MG, Oosterwijk-Wakka JC, Zegwaart-Hagemier NE, et al. Immunohistochemical analysis of tumor antigen saturation following injection of monoclonal antibody G250. *Anticancer Res* 1999;19:1197-200.
15. Steffens MG, Boerman OC, Oyen WJ, et al. Intratumoral distribution of two consecutive injections of chimeric antibody G250 in primary renal cell carcinoma: implications for fractionated dose radioimmunotherapy. *Cancer Res* 1999;59:1615-9.
16. Divgi CR, O'Donoghue JA, Welt S, et al. Phase I clinical trial with fractionated radioimmunotherapy using ¹³¹I-labeled chimeric G250 in metastatic renal cancer. *J Nucl Med* 2004;45:1412-21.
17. Goldenberg DM. Targeted therapy of cancer with radiolabeled antibodies. *J Nucl Med* 2002;43:693-713.
18. A.H. Brouwers, et al. A lack of efficacy of two consecutive treatments of radioimmunotherapy with ¹³¹I-cG250 in patients with metastasized clear cell renal cell carcinoma. In press: *J Clin Oncol* 2005.
19. Oosterwijk E, Ruiter DJ, Hoedemaeker PJ, et al. Monoclonal antibody G 250 recognizes a determinant present in renal-cell carcinoma and absent from normal kidney. *Int J Cancer* 1986;38:489-94.
20. Pastorek J, Pastorekova S, Callebaut I, et al.

- Cloning and characterization of MN, a human tumor-associated protein with a domain homologous to carbonic anhydrase and a putative helix-loop-helix DNA binding segment. *Oncogene* 1994; 9:2877–88.
21. Opavsky R, Pastorekova S, Zelnik V, et al. Human *MN/CA9* gene, a novel member of the carbonic anhydrase family: structure and exon to protein domain relationships. *Genomics* 1996;33:480–7.
 22. Grabmaier K, Vissers JL, De Weijert MC, et al. Molecular cloning and immunogenicity of renal cell carcinoma-associated antigen G250. *Int J Cancer* 2000;85:865–70.
 23. Uemura H, Nakagawa Y, Yoshida K, et al. MN/CA IX/G250 as a potential target for immunotherapy of renal cell carcinomas. *Br J Cancer* 1999;81:741–6.
 24. Pastorekova S, Parkkila S, Parkkila AK, et al. Carbonic anhydrase IX, MN/CA IX: analysis of stomach complementary DNA sequence and expression in human and rat alimentary tracts. *Gastroenterology* 1997;112:398–408.
 25. Lindmo T, Boven E, Cuttitta F, Fedorko J, Bunn PA, Jr. Determination of the immunoreactive fraction of radiolabeled monoclonal antibodies by linear extrapolation to binding at infinite antigen excess. *J Immunol Methods* 1984;72:77–89.
 26. Ebert T, Bander NH, Finstad CL, Ramsawak RD, Old LJ. Establishment and characterization of human renal cancer and normal kidney cell lines. *Cancer Res* 1990;50:5531–6.
 27. Uemura H, Okajima E, Debruyne FM, Oosterwijk E. Internal image anti-idiotypic antibodies related to renal-cell carcinoma-associated antigen G250. *Int J Cancer* 1994;56:609–14.
 28. Boerman OC, van Niekerk CC, Makkink K, Hanselaar TG, Kenemans P, Poels LG. Comparative immunohistochemical study of four monoclonal antibodies directed against ovarian carcinoma-associated antigens. *Int J Gynecol Pathol* 1991;10:15–25.
 29. Schrijvers AH, Quak JJ, Uytendinck AM, et al. MAb U36, a novel monoclonal antibody successful in immunotargeting of squamous cell carcinoma of the head and neck. *Cancer Res* 1993;53:4383–90.
 30. Buijs WC, Massuger LF, Claessens RA, Kenemans P, Corstens FH. Dosimetric evaluation of immunoscintigraphy using indium-111-labeled monoclonal antibody fragments in patients with ovarian cancer. *J Nucl Med* 1992;33:1113–20.
 31. Buijs WC, Siegel JA, Boerman OC, Corstens FH. Absolute organ activity estimated by five different methods of background correction. *J Nucl Med* 1998; 39:2167–72.
 32. Brouwers AH, Buijs WCAM, Oosterwijk E, et al. Targeting of metastatic renal cell carcinoma with the chimeric monoclonal antibody G250 labeled with ¹³¹I or ¹¹¹In: an intrapatient comparison. *Clin Cancer Res* 2003;9:3953–60s.
 33. Stabin MG. MIRDOSE: personal computer software for internal dose assessment in nuclear medicine. *J Nucl Med* 1996;37:538–46.
 34. Shen S, Meredith RF, Duan J, Brezovich IA, Khazaeli MB, LoBuglio AF. Comparison of methods for predicting myelotoxicity for non-marrow targeting I-131-antibody therapy. *Cancer Biother Radiopharm* 2003;18:209–15.
 35. Wiseman GA, White CA, Sparks RB, et al. Biodistribution and dosimetry results from a phase III prospectively randomized controlled trial of Zevalin radioimmunotherapy for low-grade, follicular, or transformed B-cell non-Hodgkin's lymphoma. *Crit Rev Oncol Hematol* 2001;39:181–94.
 36. Vose JM, Wahl RL, Saleh M, et al. Multicenter phase II study of iodine-131 tositumomab for chemotherapy-relapsed/refractory low-grade and transformed low-grade B-cell non-Hodgkin's lymphoma. *J Clin Oncol* 2000;18:1316–23.
 37. Juweid ME, Zhang CH, Blumenthal RD, Hajjar G, Sharkey RM, Goldenberg DM. Prediction of hematologic toxicity after radioimmunotherapy with (131)I-labeled anticarcinoembryonic antigen monoclonal antibodies. *J Nucl Med* 1999;40:1609–16.
 38. O'Donoghue JA, Baidoo N, Deland D, Welt S, Divgi CR, Sgouros G. Hematologic toxicity in radioimmunotherapy: dose-response relationships for I-131 labeled antibody therapy. *Cancer Biother Radiopharm* 2002; 17:435–43.
 39. DeNardo GL, Juweid M, White CA, Wiseman GA, DeNardo SJ. Role of radiation dosimetry in radioimmunotherapy planning and treatment dosing. *Crit Rev Oncol Hematol* 2001;39:203–18.
 40. DeNardo SJ, Williams LE, Leigh B, Wahl RL. Choosing an optimal radioimmunotherapy dose for clinical response. *Cancer* 2002;94:1275–86.
 41. Koral KF, Francis IR, Kroll S, Zasadny KR, Kaminski MS, Wahl RL. Volume reduction versus radiation dose for tumors in previously untreated lymphoma patients who received iodine-131 tositumomab therapy. *Cancer* 2002;94:1258–63.
 42. Koral KF, Dewaraja Y, Clarke LA, et al. Tumor-absorbed-dose estimates versus response in tositumomab therapy of previously untreated patients with follicular non-Hodgkin's lymphoma: preliminary report. *Cancer Biother Radiopharm* 2000;15:347–55.
 43. Blumenthal RD, Alisauskas R, Juweid M, Sharkey RM, Goldenberg DM. Defining the optimal spacing between repeat radioantibody doses in experimental models: is there an accurate measurement for hematopoietic recovery? *Cancer* 1997;80:2624–35.
 44. Wahl RL, Kroll S, Zasadny KR. Patient-specific whole-body dosimetry: principles and a simplified method for clinical implementation. *J Nucl Med* 1998; 39:14–20s.
 45. Chatal JF, Saccavini JC, Gestin JF, et al. Biodistribution of indium-111-labeled OC125 monoclonal antibody intraperitoneally injected into patients operated on for ovarian carcinomas. *Cancer Res* 1989;49: 3087–94.
 46. Wiseman GA, Scott AM, Lee F, Gansen DN, Hopkins W, Steinmetz S, et al. Chimeric G250 (cG250) monoclonal antibody phase I dose escalation trial in patients with advanced renal cell carcinoma (RCC). *Proc Annu Meet Am Soc Clin Oncol* 2001;20:275a.
 47. Bleumer I, Knuth A, Oosterwijk E, et al. A phase II trial of chimeric monoclonal antibody G250 for advanced renal cell carcinoma patients. *Br J Cancer* 2004;90:985–90.
 48. Colnot DR, Quak JJ, Roos JC, et al. Phase I therapy study of ¹⁸⁶Re-labeled chimeric monoclonal antibody U36 in patients with squamous cell carcinoma of the head and neck. *J Nucl Med* 2000;41: 1999–2010.

Clinical Cancer Research

Radioimmunotherapy with [¹³¹I]cG250 in Patients with Metastasized Renal Cell Cancer: Dosimetric Analysis and Immunologic Response

Adrienne H. Brouwers, Wilhelmina C.A.M. Buijs, Peter F.A. Mulders, et al.

Clin Cancer Res 2005;11:7178s-7186s.

Updated version Access the most recent version of this article at:
<http://clincancerres.aacrjournals.org/content/11/19/7178s>

Cited articles This article cites 44 articles, 16 of which you can access for free at:
<http://clincancerres.aacrjournals.org/content/11/19/7178s.full#ref-list-1>

Citing articles This article has been cited by 5 HighWire-hosted articles. Access the articles at:
<http://clincancerres.aacrjournals.org/content/11/19/7178s.full#related-urls>

E-mail alerts [Sign up to receive free email-alerts](#) related to this article or journal.

Reprints and Subscriptions To order reprints of this article or to subscribe to the journal, contact the AACR Publications Department at pubs@aacr.org.

Permissions To request permission to re-use all or part of this article, use this link
<http://clincancerres.aacrjournals.org/content/11/19/7178s>.
Click on "Request Permissions" which will take you to the Copyright Clearance Center's (CCC) Rightslink site.